



---

Magnetostratigraphic Chronology of Cretaceous-to-Eocene Thrust Belt Evolution, Central Utah, USA

Author(s): Peter J. Talling, Douglas W. Burbank, Timothy F. Lawton, Robert S. Hobbs and Steven P. Lund

Source: *The Journal of Geology*, Vol. 102, No. 2 (Mar., 1994), pp. 181-196

Published by: [The University of Chicago Press](#)

Stable URL: <http://www.jstor.org/stable/30068544>

Accessed: 30/01/2015 18:46

---

Your use of the JSTOR archive indicates your acceptance of the Terms & Conditions of Use, available at <http://www.jstor.org/page/info/about/policies/terms.jsp>

JSTOR is a not-for-profit service that helps scholars, researchers, and students discover, use, and build upon a wide range of content in a trusted digital archive. We use information technology and tools to increase productivity and facilitate new forms of scholarship. For more information about JSTOR, please contact support@jstor.org.



*The University of Chicago Press* is collaborating with JSTOR to digitize, preserve and extend access to *The Journal of Geology*.

<http://www.jstor.org>

# Magnetostratigraphic Chronology of Cretaceous-to-Eocene Thrust Belt Evolution, Central Utah, USA<sup>1</sup>

*Peter J. Talling,<sup>2</sup> Douglas W. Burbank, Timothy F. Lawton,<sup>3</sup>  
Robert S. Hobbs,<sup>4</sup> and Steven P. Lund*

*University of Southern California, Los Angeles, CA 90089-0740, USA*

## ABSTRACT

The Axhandle basin in central Utah is a piggyback basin that formed above the Gunnison thrust system. The basin contains ~1 km of upper Cretaceous-to-Eocene strata of the North Horn and lower Flagstaff Limestone formations. A significantly more exact chronology, based on magnetic polarity stratigraphy, has been developed for the basin-filling strata. The new data provide a detailed temporal framework for the interpretation of the depositional and tectonic evolution of the basin during chrons 33–21 (~75–49 Ma). Tectonic subsidence curves and stratigraphic relations along the eastern basin margin define two episodes of motion on the Gunnison thrust system. The majority of tectonic shortening on the system occurred between 83–75 Ma and caused widespread non-deposition within the Axhandle basin. A second episode of motion, in detail comprising of four separate periods of backthrusting, occurred between 70–60 Ma. The Canyon Range, Pavant, and Nebo thrust sheets were emplaced 30–50 km to the west of the Axhandle basin between 97 and 74 Ma. The initial episode of motion on the Gunnison thrust system was thus partly coeval with the emplacement of these thrust sheets. Uplift and erosion above the San Rafael Swell, a basement flexure located ~100 km east of the Axhandle basin, occurred at the same time—between 70 and ~60 Ma—as the second episode of motion on the Gunnison thrust system. These age constraints clearly demonstrate coeval motion on multiple contractional structures. Episodes of thrust wedge reorganization with durations of 5–10 m.y. appear to be separated by quiescent periods of up to 5 m.y. Evolution of the thrust belt in NE Utah and Wyoming was remarkably similar to that in central Utah 300 km to their south. This similarity suggests that the tectonic stresses driving the thrust wedge were relatively uniform along strike.

## Introduction

Piggyback basins formed above active thrust faults have the potential to provide a detailed record of the evolution of the underlying thrust system. In the absence of reliable chronologies, however, the temporal spacing of these events, the duration of gaps in the record, and the rates of processes remain largely unknown. Terrestrial strata are often characterized by a sparse fossil record and a paucity of strata suitable for isotopic age determinations. In such situations, chronologies based on magnetic polarity stratigraphy can provide the requisite tem-

poral constraints. We describe here the results and implications of recent magnetostratigraphic studies for the evolution of the Axhandle piggyback basin, and the underlying, episodically active Gunnison thrust system in central Utah (figure 1). The history of the Gunnison thrust system forms a critical part of an evolution in Central Utah, from thin-skinned thrusting to basement-involved uplifts.

In this study, magnetic polarity stratigraphies have been obtained for three stratigraphic sections located in close proximity to the eastern, back-thrusted basin margin. The resulting chronology is used to constrain the evolution of the basin-filling deposystems, the detailed history of uplift of the eastern, basin-margin backthrust, and the temporal pattern of rates of sediment accumulation and inferred subsidence within the basin.

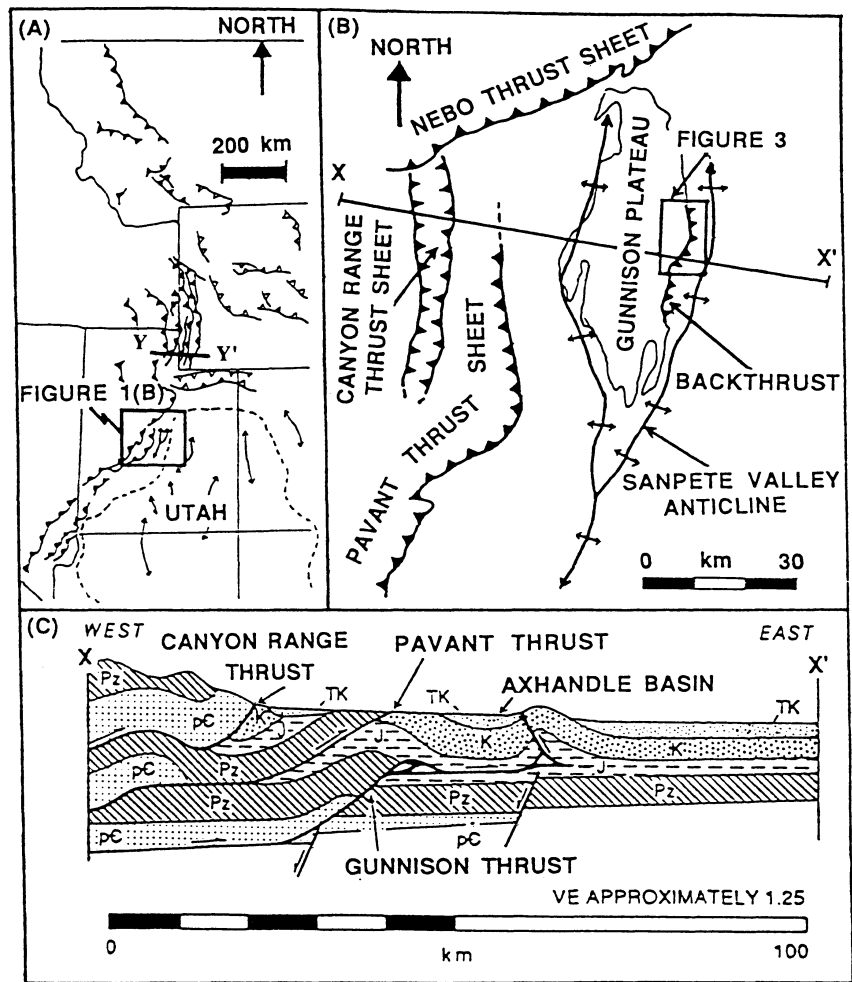
<sup>1</sup> Manuscript received March 15, 1993; accepted November 11, 1993.

<sup>2</sup> Present address: Leeds University, Leeds, LS2 9JT, U.K.

<sup>3</sup> New Mexico State University, Las Cruces, NM 88003, USA.

<sup>4</sup> Exxon Petroleum Company, Houston, TX 77210-4279, USA.

**Figure 1.** (a) Location of the study area in central Utah. The location of the cross section in NE Utah and SW Wyoming shown in figure 12b is indicated by Y-Y'. (b) Map of the major structural elements of Central Utah in Late Cretaceous and Early Tertiary time. The Axhandle basin, defined by a hangingwall-ramp anticline on the west and a west verging backthrust structure on the east, is roughly coincident with the present day Gunnison Plateau. The area shown in more detail in figure 2 is boxed. (c) Generalized E-W structural cross section across central Utah, after Lawton and Trexler (1991). The location of this cross section, and the cross section shown in figure 12a, is indicated by X-X' in figure 1b. Pz = Paleozoic strata; pe = Precambrian sedimentary strata; J = Jurassic and Lower Cretaceous strata; K = Indianola Group; TK = North Horn Formation.



### Local Description

The 30-km-wide Axhandle basin was produced by thrust disruption and partitioning of the proximal Sevier foreland during the latest Cretaceous to early Tertiary (Lawton and Trexler 1991). The basin is defined by a hangingwall-ramp anticline to the west and a W-verging backthrust structure to the east. The two structures are connected by an inferred thrust flat that underlies the basin (figure 1; Lawton et al. 1994; Villien and Kliegfield 1986; Lawton and Trexler 1991). Along the eastern escarpment of the present-day Gunnison Plateau (figure 2), the basin-filling, alluvial, and lacustrine strata assigned to the North Horn and lowermost Flagstaff Limestone formations (figure 3) are well exposed. Stratigraphic relations, such as angular and progressive unconformities, paleocurrent reversals, and ponding of alluvial deposystems, show that the backthrust was episodically active during deposition of these strata (figure 3; Lawton and

Trexler 1991; Talling 1992). Prior to this study, however, the chronology of deposition and deformation has only been loosely defined.

### Methods and Remnant Characteristics

At each site in the three sections (figure 2), 3–4 oriented samples were collected from siltstone, limestone, or mudstone. The sampling procedure was similar to that of Johnson et al. (1975). Sections were measured using a Jacob's staff and Abney level. A site spacing of 5–8 m was typically achieved. In an attempt to clarify ambiguous areas of polarity stratigraphy, the Axhandle Canyon section, with 94 sites, and the Petes Canyon section, with 140 sites, were intensively resampled on two occasions subsequent to their initial sampling. Hobbs (1989) provides an interpretation of the data available after an initial set of resampling. The Boiler Canyon section, with 41 sites, was only

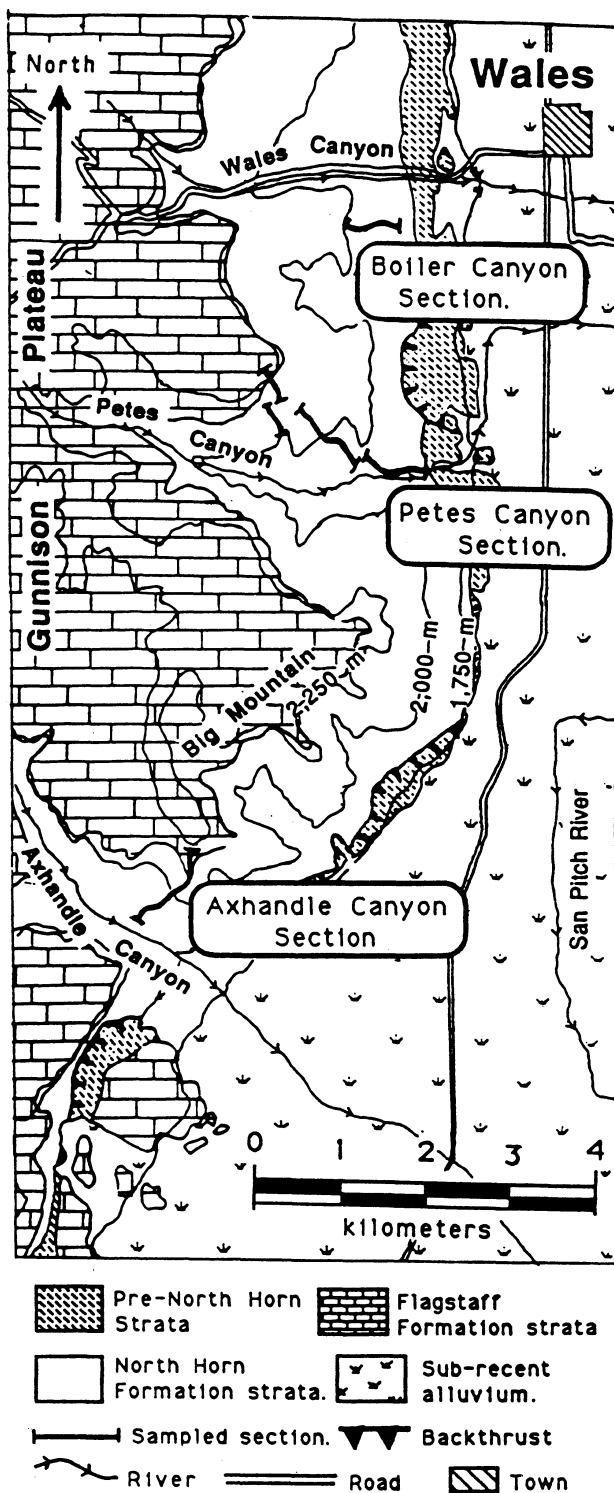


Figure 2. Simplified geologic map of the eastern escarpment of the Gunnison Plateau showing the localities of the Axhandle Canyon, Petes Canyon, and Boiler Canyon sections.

sampled once, and thus its polarity stratigraphy is less well defined. Marker beds were used to correlate the three individual sections to produce a single, composite magnetic polarity stratigraphy.

A combination of laboratory unblocking-temperature spectra, alternating-field coercivity spectra, and acquisition and thermal demagnetization of isothermal remnant magnetization (IRM) was utilized to investigate the magnetic mineral phases present. Within the North Horn Formation, abrupt facies changes, together with paleopedogenic evidence of a fluctuating water table (figure 3), suggest that there was potential for forming both authigenic and detrital mineral suites. The finite number of pilot samples demagnetized in detail necessarily underestimate the variety of these mineral suites.

The Natural Remnant Magnetism (NRM) of most rock types is characteristically weak, particularly in the calcareous mudstones of the Petes Canyon section. Intensities of  $1 \times 10^{-3}$  to  $2 \times 10^{-4}$  A/m are common and begin to approach the sensitivity of the cryogenic magnetometer. Weakly magnetized samples often provided inconsistent demagnetization behavior at the site level. Such sites, which constituted 31% of the total, were not used in generating polarity stratigraphies. A weak signal is also noted in the only previous paleomagnetic study of North Horn Formation deposits, at the type section 50 km east of the Gunnison Plateau (Tomida and Butler 1980). The regionally low magnetic intensities may be related in part to a lack of volcanic input and to source area dominance by carbonate-rich strata.

Laboratory unblocking-temperature spectra suggest that there are three major components contributing to the magnetic signal (figure 4a,b,c). These are (a) a component removed by 150–250°C, (b) one removed between 150–250°C and 450–550°C, and (c) a component removed above 550°C. Often all three components are present in the same sample. The respective laboratory unblocking temperatures of the three components suggest that (a) is goethite, (b) is titanomagnetite or magnetite, and (c) is hematite.

A limited number of alternating-field demagnetization results display only two clear components. These components have coercivities of (a) <25 mT, and (b) 25–80 mT (figure 4d, and Hobbs 1989). These coercivities also support the presence of the goethite and of the titanomagnetite or magnetite components.

IRM acquisition data also provide evidence of variable mineralogies. Sample PC602 shows saturation of the induced signal occurring by 300 mT

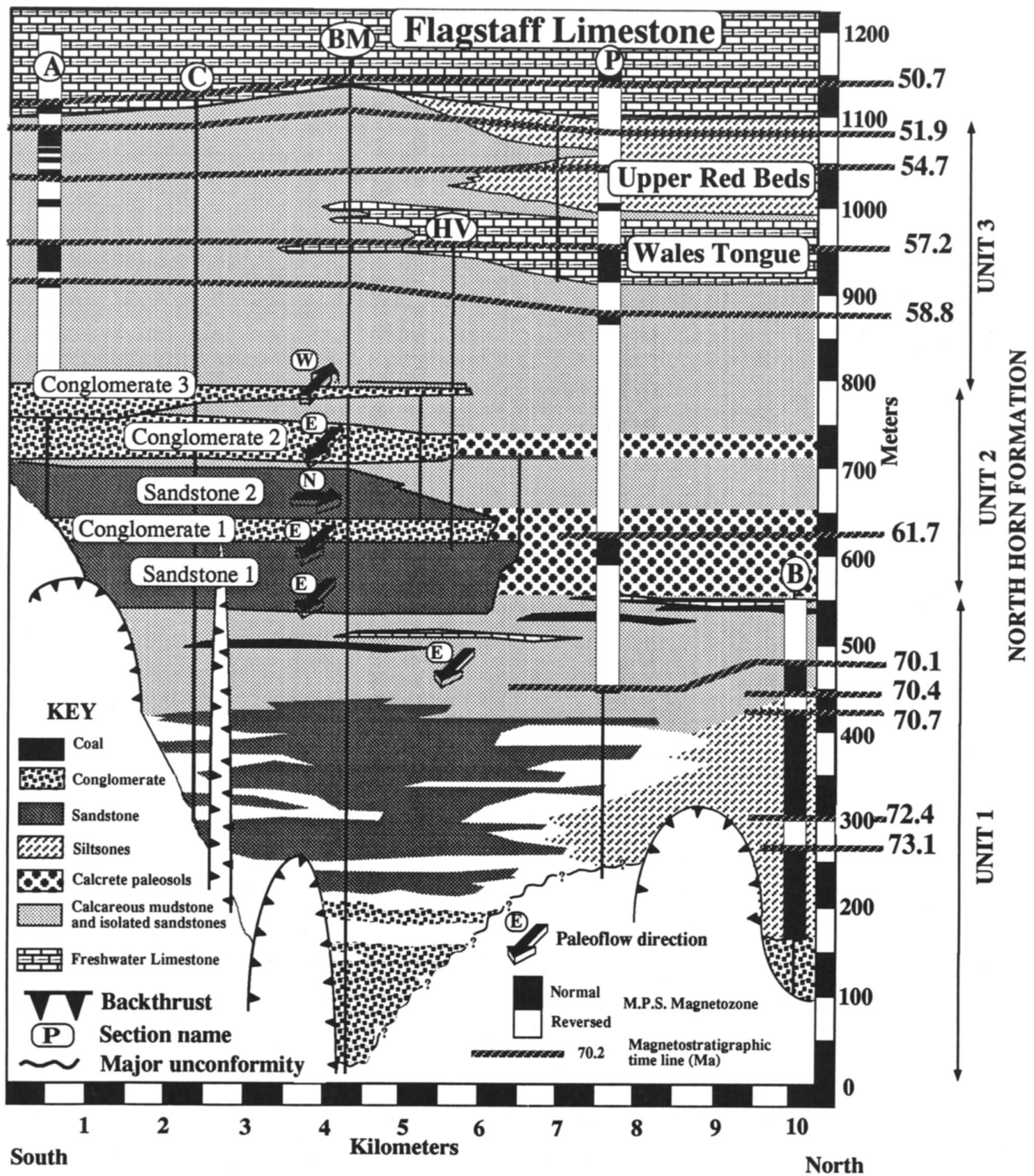


**Figure 3.** N-S stratigraphic cross section along the eastern escarpment of the Gunnison Plateau, showing the character of North Horn strata adjacent to the eastern margin of the Axhandle basin. Stratal subunits, paleocurrent directions (shown with respect to the N-S orientation of the panel), and stratigraphic relations that constrain the relative timing on the basin-margin backthrust (backthrusts are indicated by the barbed symbol) are depicted. Paleocurrent data is outlined in Talling (1992). Detailed correlations are based on lateral tracing of individual strata and matching of magnetozone boundaries. Ages on the right side are taken from the Harland et al. (1990) time scale. Three magnetic polarity stratigraphies were sampled from the Axhandle Canyon (A), Petes Canyon (P), and Boiler Canyon (B) sections. Other measured and described sections (C = Coal Canyon; BM = Big Mountain; and HV = Hanging Valley) were used in the stratigraphic correlations but were not sampled for magnetic studies.

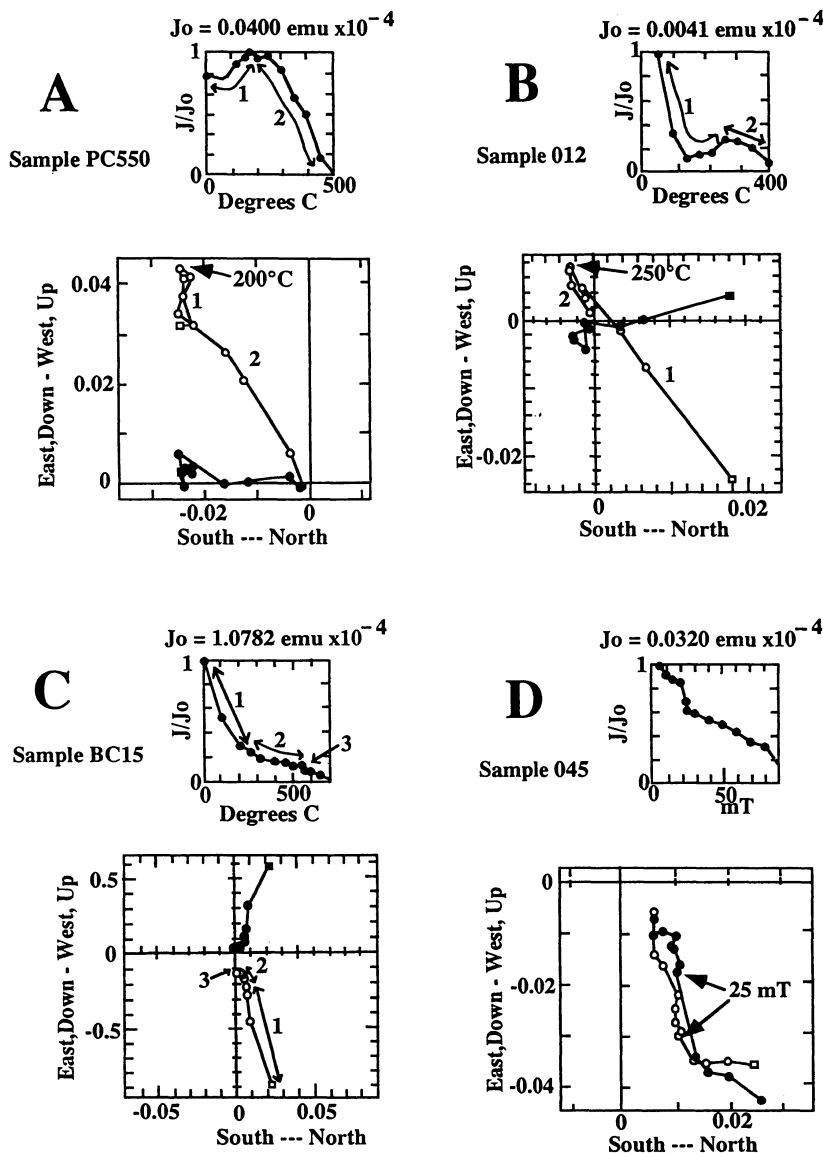


**Figure 4.** Representative Zijdeveld plots (Zijderveld 1967) of stepwise thermal and alternating field demagnetization and of associated intensity changes. (a) Reversely magnetized specimen showing two components: one removed below 175°C and a second, presumed to be carried by titanomagnetite, removed between 200–500°C. (b) Reversely magnetized specimen showing a component removed below 250°C, and a second component largely removed by 400°C. (c) Normal polarity specimen from the lower part of the Boiler Canyon section exhibiting 3 components: 25–200°C, 200–550°C, and >550°C. The high temperature component is likely to be hematite. (d) Plot of alternating-field demagnetization of a normally magnetized specimen, showing rapid intensity loss below 25 mT, and steady loss between 25 and 90 mT. Any hematite overprint is minimal.

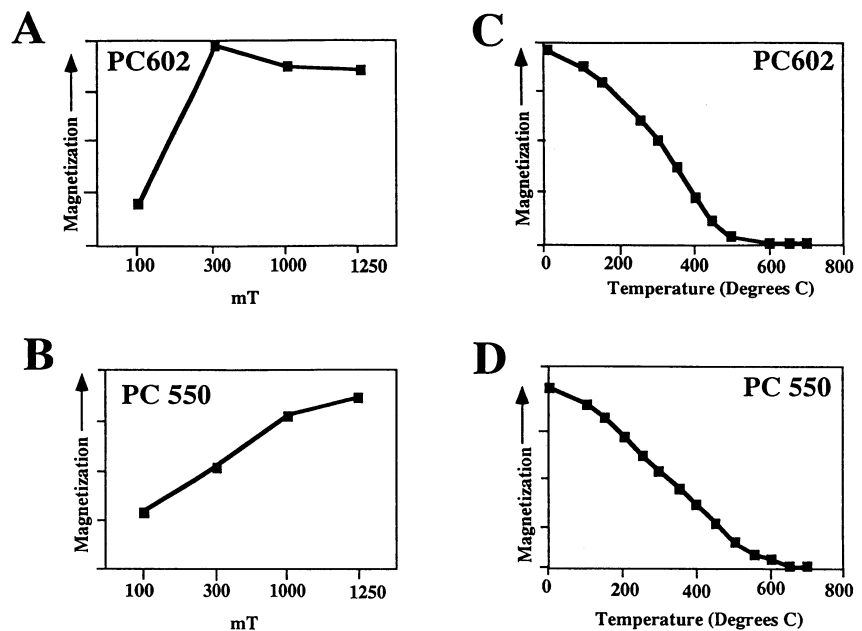
(figure 5a). This suggests a relatively low coercivity magnetite or titanomagnetite phase. Many other specimens, however, display only partial saturation at imposed field strengths of 1.25 T (figure 5b). This suggests a mixture of low and high coercivity components, with the higher coercivity component being hematite or possibly goethite.

Stepwise thermal demagnetization of the saturation or partial-saturation IRM confirms the presence of two components, one with blocking temperatures of 150–500°C and the other with blocking temperatures of 600–675°C (figure 5d,e,f). The former represents the titanomagnetite or magnetite and the latter the hematite component.

Some stratigraphic intervals sampled display a

consistently distinct magnetic signal character. The lower part of the Boiler Canyon section (below meter 250) comprises orange-brown mottled siltstone and local conglomerate. These rocks are strongly magnetized, and intensities of  $1 \times 10^{-2}$  A/m are common. Laboratory unblocking-temperature spectra of samples in this interval range between 200–550°C, suggesting the presence of magnetite as the primary magnetic carrier (figure 4c). Calcareous, grey mudstone typically contained the lowest NRM intensities, with the relatively pure micrites of the Wales Tongue (figure 3) producing a particularly weak signal. Resampling of less resistant strata adjacent to previously sampled resistant calcareous muds or impure micrites failed

**Figure 5.** Isothermal remnant magnetization (IRM) acquisition of pilot samples. (a) PC602 shows saturation by 300 mT suggesting a titanomagnetite or magnetite component. (b) PC550 displays only partial saturation by 1.25 T suggesting a high coercivity magnetic phase, presumably hematite, in addition to the titanomagnetite or magnetite. (c)–d. Thermal demagnetization of saturation IRM. (c) PC602 shows no significant remnance above 580°C, indicating an absence of hematite as is also suggested by the IRM acquisition curve (a above). (d) Minor remnance remains above 580°C indicating some hematite in PC550.



to improve the quality of the paleomagnetic data significantly. The lower part of the Axhandle Canyon section (0–190 m, figure 6) is laterally equivalent to meters 340–500 in the Petes Canyon section (figure 7). The Axhandle Canyon samples, however, displayed consistently higher NRM intensities and a higher percentage of Class 1 sites (figures 6 and 7). Because this trend appears to be largely independent of lithology, we speculate that the Axhandle section was closer to the basin margin and received a higher terrigenous detrital input.

The strata that yielded the most consistent results were orange- or red-stained siltstone and mudstones containing a high intensity hematite component. However, because the timing of that hematite component is poorly constrained, the polarity calculations obtained from these hematite-bearing strata are considered equivocal.

**Measurement Strategy.** This study attempted to isolate the remnance direction of the titanomagnetite or magnetite component of assumed detrital origin. The hematite component, in contrast, is more likely to be authigenic, and postdates deposition by some unknown time. Following the pilot studies, all remaining samples were stepwise thermally demagnetized between 200° and 350°C. The resulting magnetization directions at each site were averaged using 3–4 specimens at a single temperature step. Fisher (1953) statistics were used to assess the directional coherence at each site. Sites with a Fisher  $k$  of  $>10$  are termed Class 1. Sites with a Fisher  $k$  of  $<10$ , but with unambigu-

ous normal or reversed polarity, were termed Class 2 sites. Class 1 sites with anomalous magnetic character, such as those 100 times stronger than average, were demoted to Class 2. Sites with no coherent magnetic directions were defined as Class 3 and rejected. Of the total of 275 sites, 45% were Class 1, 24% were Class 2, and 31% were Class 3. The site mean directions were converted to virtual geomagnetic pole (VGP) positions based on a paleolatitude and paleolongitude of 39°N, 249°E (figures 6–8). A magnetozone was defined for the local magnetostratigraphies when indicated by at least one Class 1 site, with the exception of two reversed polarity magnetozone in the lower Boiler Canyon section (figure 8) that contain only Class 2 sites. These sites were interpreted as showing a convincing reversed polarity.

**Timing of Magnetic Signal Acquisition.** The titanomagnetite component is considered detrital in origin and should have been locked in following burial below the depth of bioturbation, i.e., within several thousand years after deposition. The hematite component could have been acquired authigenically at any time up to the present. Because demagnetization between 200° and 350°C does not unblock the hematite signal, the measured directions may include a hematite overprint of uncertain magnitude. In many cases Zijderveld diagrams were used to distinguish these components (Zijderveld 1967; figure 4c). The class 1 data pass the reversal test at the 95% confidence level (Appendix 1, available from *The Journal of Geology*, free of

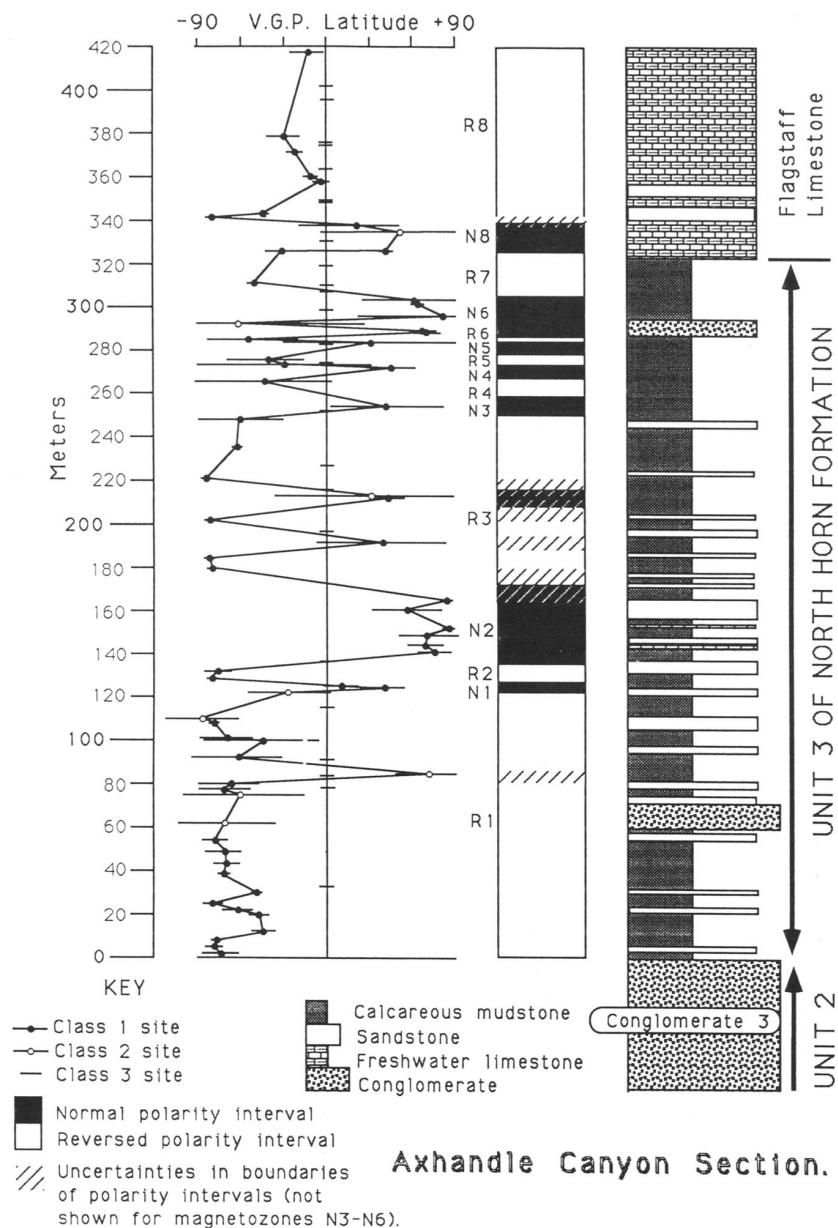


**Figure 6.** Polarity stratigraphy for the Axhandle Canyon section. For this and subsequent figures, Class 1 and 2 sites are shown by closed and open dots, respectively. Error bars (alpha 95) on the virtual geomagnetic pole latitudes represent the calculated 95% confidence limit from the mean direction, expressed as an angular radius. Lithologies, major stratigraphic units, stratigraphic contacts, and the numbering used to delineate magnetozones (R1–R8) are shown. Uncertainties in magnetozone boundaries result from the separation between superposed sites and less well documented magnetozones based on Class 2 sites. Class 3 sites rejected for polarity assignments are marked in their appropriate stratigraphic position along the 0° VGP line.

charge) and define VGP positions compatible with a Paleocene pole position of 81.5°N, 192.6°E (Diehl et al. 1988).

Although it is possible that post-depositional overprinting by hematite could have obscured the original detrital signal in some cases, the repeated occurrence of lithologically independent magnetozones of consistent polarity, the presence of reversal boundaries within apparently homogeneous lithological units, and the replication of polarity patterns between stratigraphically correlative parts of spatially separated sections (except as noted below) strongly suggests that the polarity pattern de-

veloped here closely mimics field polarity as recorded at the time of deposition.

**Results.** Despite uncertainties related to weak sample intensities and the age of acquisition of the hematite-dominated remnance, the three sampled sections produce a series of both normal and reversed polarity zones typically defined by several sites (figures 6–8). A single composite polarity stratigraphy was produced for the North Horn Formation by correlating the three individual stratigraphies (figure 9). Correlation was achieved with confidence of ± 10 m using traceable marker beds (figures 3 and 9). An instructive test of the reliabil-

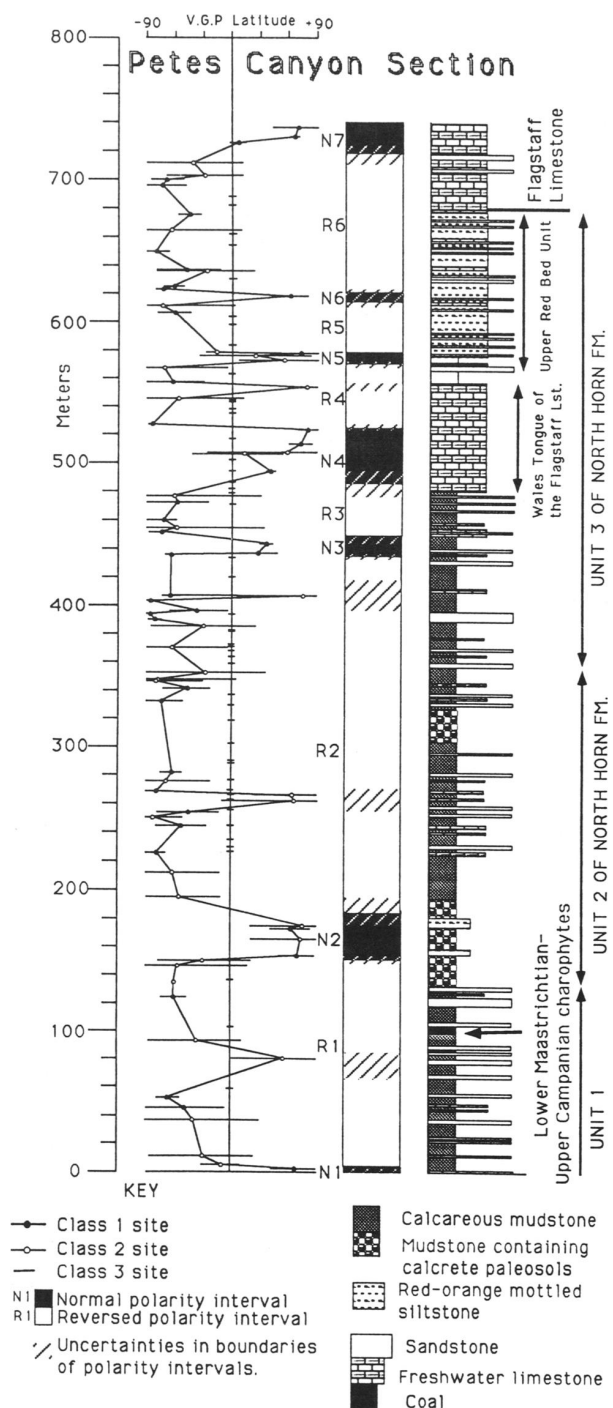


**Figure 7.** Polarity stratigraphy for the Petes Canyon section. Stratigraphic position of charophyte site is shown. Description is the same as for figure 6.

ity of the composite polarity stratigraphy is provided by the overlaps between laterally adjacent sections. The lower part of the overlap between the Petes Canyon and Axhandle Canyon sections is in good agreement, with a well defined normal chron and a longer reversed interval (chrons N4 and R4, figure 9), whereas the complex reversal pattern in the upper half of the Axhandle section (chrons N8 to N12, figure 9) is not reproduced in the Petes Canyon section. This suggests that either (a) the normal chrons in the Axhandle section are secondary magnetizations, (b) the reversed signal in the Petes Canyon section is an overprint, or (c) that the Petes Canyon section contains a significant unconformity. This part of the Petes Canyon section comprises a series of red-to-orange mottled coarse siltstone beds (the Upper Red Bed unit; figures 3 and 9). It thus is speculatively suggested that the red-orange mottling indicates the presence of a hematite overprint.

**Correlation to the Global Magnetopolarity Time Scale.** The correlation is initially constrained by independent, biostratigraphic, or radiometric dating of the strata. Regionally the North Horn Formation is dated as Maastrichtian to early Eocene based on fossil localities east of the Gunnison Plateau. The type section, 50 km east of the Gunnison Plateau, contains Late Cretaceous vertebrates and invertebrates (Gilmour, in Spieker 1949), Puercan and Torrejonian (Paleocene) mammal faunas (Tomida and Butler 1980), and Late Cretaceous palynomorphs (Greisbach and McAlpine 1973). Other North Horn exposures on the Wasatch Plateau have yielded Maastrichtian palynomorphs (Standlee 1982; Schwanns, 1988) and mid-to-late Paleocene calcareous microfossils and palynomorphs (Fouch et al. 1982). On the Gunnison Plateau, a coal in the Petes Canyon section (meter 100, figure 7) in the lower part of the North Horn strata has yielded a tentative Late Campanian to early Maastrichtian date based on an ostracod assemblage (R. M. Forester pers. comm. 1989). The absence of *Platychara compressa* in the Axhandle basin strata, common in late Maastrichtian times, is cited as evidence of a pre-late Maastrichtian age. Schwanns (1988) lists Maastrichtian palynomorphs collected at the coal in the Petes Canyon section. Undifferentiated dinosaurian remains found at two localities (meters 90 and 165, figure 8) in the Boiler Canyon section indicate a pre-Paleocene age for those North Horn strata (Lawton et al. 1994).

The Flagstaff Limestone regionally overlies the North Horn Formation and is present at the tops of the Axhandle Canyon and Petes Canyon sections. It is dated regionally as Late Paleocene to

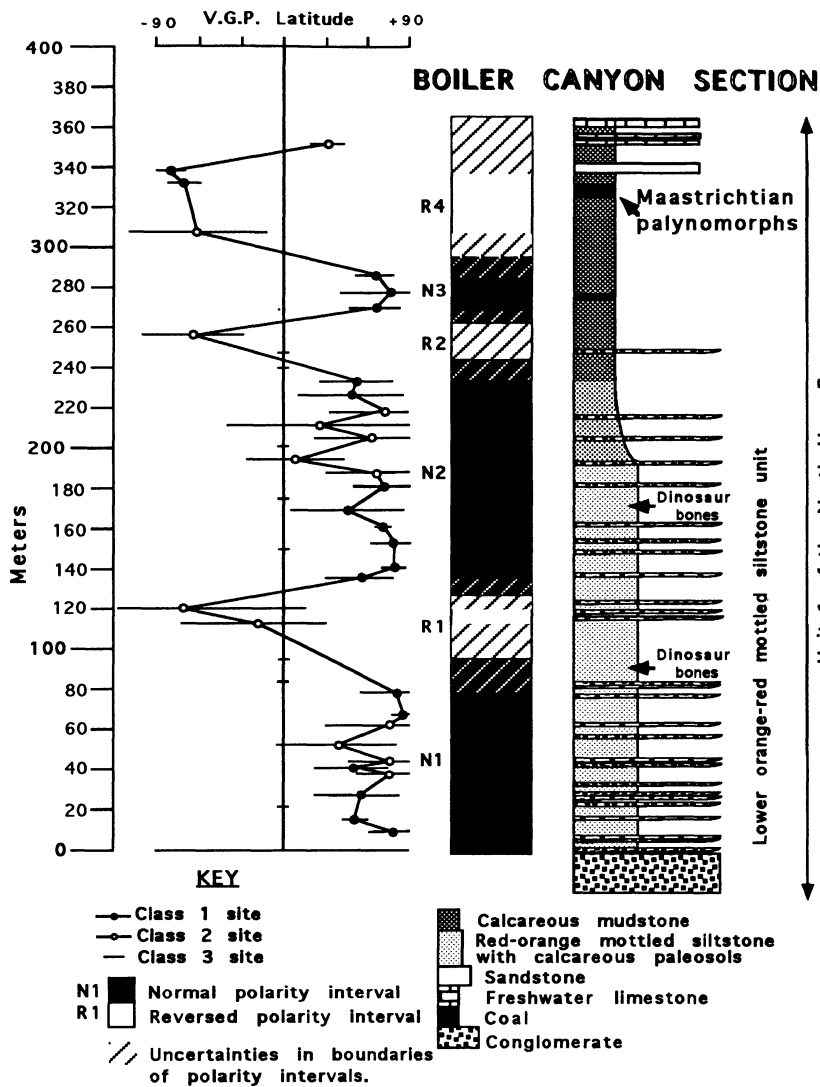


Figure 8. Polarity stratigraphy for the Boiler Canyon section. Stratigraphic positions of dinosaur fossils are shown. Description is the same as for figure 6.

Early Eocene, based on molluscs (La Rocque 1960), charophytes (Peck and Reker 1948), a mammal jaw bone found in float (Rich and Collinson 1973), and pollen (Fouch et al. 1982). On the Gunnison Plateau, mollusc assemblages suggest that the basal of three regionally recognized informal members of the Flagstaff Limestone is absent, and an early Eocene age is estimated (La Rocque 1960).

These independent age controls place (a) the local transition from the North Horn Formation to the Flagstaff Limestone in the early Eocene and (b) the Cretaceous-Tertiary boundary stratigraphically above the coals at Petes Canyon (meter 100) and Boiler Canyon (meter 330). In the context of these biostratigraphic constraints, the optimal correlation of the composite magnetic polarity pattern to the global magnetic polarity time scale (Harland

et al. 1990) spans from chrons C33 to C21 (figure 10), and provides a reasonable match for the complex reversal pattern of chrons 23 and 24. One of the normal magnetozones (N7, figure 10) has no correlative in the Harland et al. (1990) time scale. It may correspond with one of the seven cryptochrons delineated in this part (chron 24R) of the magnetic record by Cande and Kent (1992).

The preferred correlation suggests a major depositional hiatus or erosional unconformity in late Maastrichtian and early Paleocene time. Centimeter-scale observation of the relevant part of the Petes Canyon section does not clearly reveal such major disconformities (Talling 1992). This interval does contain two zones of stacked, early stage 3 (terminology of Gile et al. 1966) calcrete paleosols (figure 7). Such paleosol formation, however,

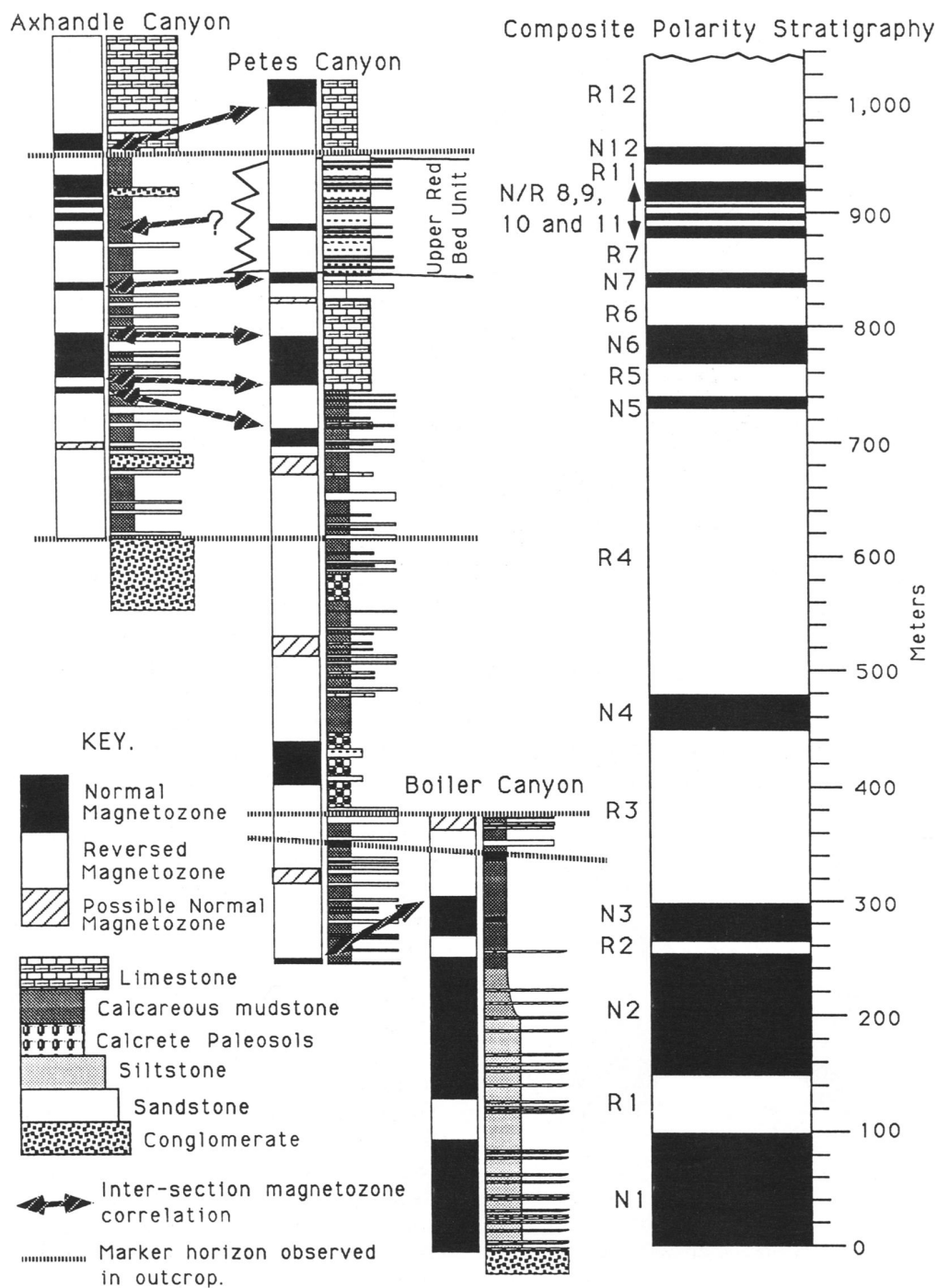


**Figure 9.** Composite magnetopolarity stratigraphy for the North Horn and lower Flagstaff Limestone Formations, derived from correlation of the three local magnetopolarity stratigraphies (figures 6–8). The stratal thicknesses of magnetozones N1–N3 are taken from the Boiler Canyon section, thicknesses of N5–N6 are averaged from the Axhandle and Petes Canyon sections, and thicknesses of R6–R12 are taken from the Axhandle Canyon section. Correlation between sections was achieved to within  $\pm 10$  m using panoramic photographic mosaics and marker beds that were physically traced out.

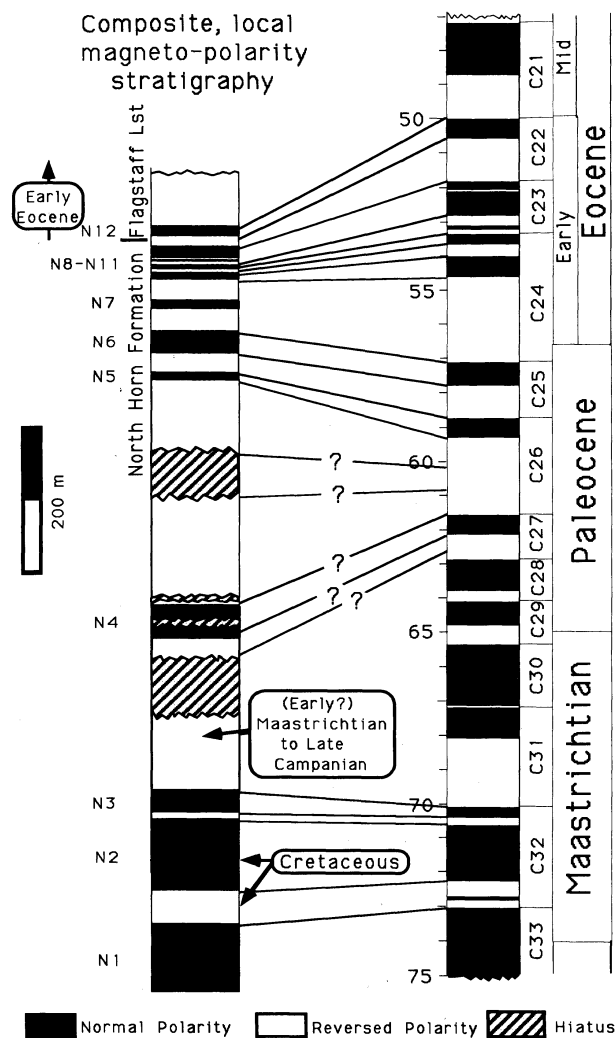


**Figure 10.** Preferred correlation of the composite magnetopolarity stratigraphy to the global magnetopolarity time scale (Harland et al. 1990), that is most reasonable given the biostratigraphic constraints indicated. Intervals with diagonal shading represent likely unconformities implied by this correlation. Unconformities of the durations indicated are problematic to document from outcrop observations; however, the unconformities are inferred to lie within two zones of calcrete paleosols (meters 130–195 and meters 315–335 of figure 7). Details of the correlation of polarity intervals between inferred unconformities are uncertain. One uncorrelated magnetozone occurs within that part of the local magnetic stratigraphy that is correlated with chron 24r. This probably represents one of the several cryptochrons recently defined in this interval (Cande and Kent 1992).

should encompass only a small fraction of the apparent >5 m.y. gap in the record. The magnetostratigraphic evidence for such an unconformity is strong, given the Maastrichtian age of the lower section, such that even the less favored correlations require a significant hiatus (figure 10; Talling and Burbank 1993). It is thus inferred that a subtle disconformity within the paleosols marks the extensive hiatus. Although various alternative correlations can be proposed and serve to illustrate the uncertainties involved in the preferred correlation, each of them violates one or more of the biostratigraphic age constraints or seems to require highly variable and improbable sediment-accumulation rates. A more thorough discussion of alternative correlations is provided in Talling and Burbank (1993).

### Implications of the Magnetostratigraphic Dating

The stratal ages reported here typically have uncertainties of  $\pm 0.5$  m.y., from inexact placement of events within a polarity chron and the sometimes arbitrary nature of formational boundaries in outcrop (Talling and Burbank 1993). The transition from the North Horn Formation to the overlying Flagstaff Limestone Formation occurs in the reversed part of chron 22 (figure 10), i.e., at  $51 \pm 0.5$  Ma. Such an age (latest Ypresian) suggests that the upper part of the North Horn Formation is temporally equivalent to the lowest member of the Flagstaff Limestone Formation elsewhere in the region (Stanley and Collinson 1979), as deduced by La Rocque (1960) from molluscan faunas. The Wales Tongue of the Flagstaff Limestone, which inter-fingers with the upper North Horn strata on the Gunnison Plateau (figure 3), occurs in the normal part of chron 25 and the base of the reversed part of chron 26 (figure 10), i.e.,  $58\text{--}56 \pm 0.5$  Ma or latest Paleocene. The Wales Tongue thus appears to be the representation on the Gunnison Plateau of the Ferroan Mountain Member (Stanley and Collinson 1979), the lowest regionally recognized member of the Flagstaff Limestone Formation. The oldest North Horn Formation strata sampled correlate to the normal part of chron 33 (figure 10). This demonstrates that the base of the North Horn predates 73.1 Ma and is thus earliest Maastrichtian or more probably latest Campanian in age.

### Evolution of the Gunnison Thrust System

The first period of uplift on the eastern, basin-margin backthrust is deduced from a series of rotated unconformities in conglomerates in the low-

est part of the North Horn Formation (Lawton et al. 1994; Lawton and Trexler 1991) below the base of the sampled sections, and from substantial erosion (>2 km) and deformation of Cretaceous units underlying the North Horn Formation (Lawton et al. 1994). This deformational episode accounts for most of the 2–5 km of shortening on the backthrust structure (Lawton 1985), with later episodes representing relatively minor structural re-activation. Magnetostratigraphic dating implies this episode predates 75 Ma, i.e., the middle of normal chron 33 (figure 10). Faulting associated with this episode displaced rocks dated biostratigraphically as latest Santonian to Middle Campanian in age (Lawton et al. 1994; Lawton and Trexler 1991). The deformation thus occurred between 83 and 75 Ma.

A second episode of uplift is inferred from strata dominated by poorly oxidized overbank deposits associated with coals and thin limestones (figure 3, meters 250–380). These strata are interpreted to represent a near-surface water table. When rivers drain from the downthrown footwall of a thrust fault, and across an upthrown hangingwall, a high water table is predicted in the area of the upstream footwall. This high water table or “ponding” results from impedance of groundwater flow by topography (Freeze and Witherspoon 1967) and by the formation of lakes during individual seismic-uplift events. The area presently upstream of the El Asnam thrust fault in northern Algeria represents a clear modern analog of such a situation (Meghroui et al. 1988). Paleoflow indicators in this ponded interval in the fill of the Axhandle basin demonstrate eastward paleoflow (figure 3) across the backthrust-uplift (figure 1), which is consistent with the scenario of the depositional model. This ponded interval is dated as 71–69 Ma (figure 10), from normal chron 32.2 to the early-to-middle part of the reversed part of chron 31. A third period of uplift, occurring at least at one locality along the backthrust’s strike, is clearly demonstrated by a progressive unconformity in “Sandstone 1” (Talling 1992; figure 3) that implies ~100 m of uplift of the eastern basin margin. This episode cannot be dated precisely from the magnetostratigraphies due to the inferred presence of major unconformities above and below it. The episode must, however, have occurred between 68.5 and 61.5 Ma (figure 10). A fourth uplift episode is inferred from strata interpreted to have been deposited by structurally ponded deposystems (figure 10, meters 430–560) with eastward paleoflow directions analogous to episode 2. This deformation probably oc-

curred between 61.5 and 60.5 Ma (i.e., the middle of the reversed part of chron 26), although, if a large unconformity is inferred above these strata, it may be as old as 64.2 Ma. A final episode of uplift is demonstrated by a 180° rotation of paleocurrent directions (figure 3, meters 780–800; figure 10, meters 590–610). This uplift is dated as between 61 and 59.5 Ma (mid-to-upper part of chron 26r; figure 10).

Although the lacustrine Wales Tongue interval may also represent the effects of structural ponding, its correlation to the lower member of the Flagstaff Limestone suggests such ponding was a regional feature and not a product of uplift on the Sanpete Valley anticline. A minor influx of conglomerate into the basin, shortly before the North Horn to Flagstaff Limestone transition, is represented by <10 m thick conglomeratic deltaforesets in the Axhandle section. Due to the localized and thin nature of these conglomerates, and uncertainties over climatic and sediment source area variation, a separate interval of uplift is not inferred from these conglomerates.

It thus appears that the eastern basin margin backthrust ceased actively uplifting around  $60 \pm 0.5$  Ma after undergoing at least five episodes of uplift over a period of 14.5–23.5 m.y. The magnitude of erosion associated with the first episode of uplift between 83 and 75 Ma suggests that the majority of shortening occurred during this period.

#### Rates of Sediment Accumulation and Tectonic Subsidence

Decompacted sediment accumulation rates show significant variability, with values of between ~25 and 1.5 cm/ka (figure 11a). This variability is despite the fact that the preferred correlation of the Axhandle basin polarity stratigraphy to the geopolarity time scale implicitly discriminates against rapid variations in accumulation rates (Talling and Burbank 1993). Accumulation rates do, however, demonstrate a general trend of decreasing values. A tectonic subsidence curve for the basin, calculated by the methods of Sclater and Christie (1980) (in Angevine et al. 1988; Allen and Allen 1990) shows that tectonic subsidence decreased with time (figure 11b). Superimposed on this trend are two periods of reduced or negative tectonic subsidence that correlate with periods of reduced sediment accumulation (figure 11a). These periods also correlate strongly with the previously outlined, independent stratigraphic evidence of thrust-induced uplift, such as angular and progressive unconformi-

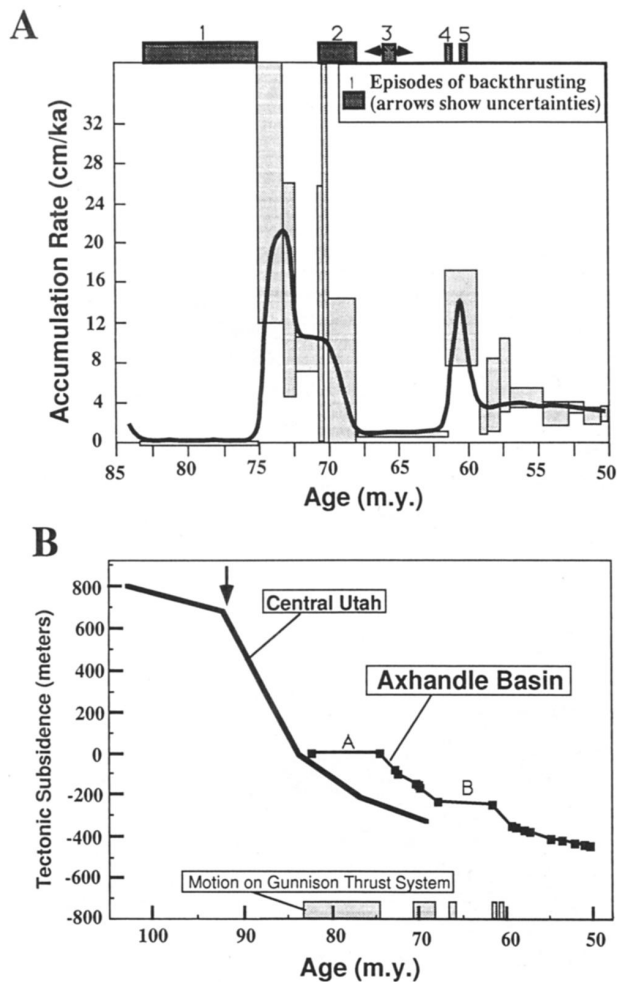


**Figure 11.** (a) Plot of decompacted sediment accumulation rates through time, defined by the preferred correlation of the local composite magnetostratigraphy to the global magnetic polarity time scale. The error envelope is defined by the spatial uncertainties, due to the finite spacing of samples, in the position of individual magnetozones boundaries of the local magnetostratigraphy. Other potential errors such as inaccuracies in measurement of stratal thicknesses ( $\pm 5\%$ ), or in the global time scale are not considered. The stratigraphically defined timing of intervals of backthrusting (stippled bars) is shown. (b) Tectonic subsidence curves calculated for the Petes Canyon section following the methods of Sclater and Christie (1980) as shown in Angevine et al. (1988) and Allen and Allen (1990). Superimposed on a declining subsidence rate are two periods of reduced subsidence labeled A and B. These periods are inferred to represent episodes of structural uplift on the Gunnison thrust system. The timing of stratigraphically defined intervals of backthrusting (stippled bars) are shown. The central Utah tectonic subsidence curve is based on data from localities outside the Axhandle basin (after Heller et al. 1986).

ties, ponded deposystems, and reversed paleoflow directions (figure 11). It is inferred that the smooth, decreasing trend results from flexural response to lithospheric loading by thrust sheets, and that the two anomalous episodes are produced by localized thrust-induced uplift. Anomalous periods of reduced tectonic subsidence may be inferred if the topographic elevation of deposition in the basin significantly increased (Sclater and Christie 1980). This is most likely to occur if the basin became internally drained. There is no sedimentary or paleocurrent evidence that internal drainage occurred in the Axhandle basin during these episodes. The tectonic subsidence plot suggests that uplift on the Gunnison thrust system occurred in two distinct episodes separated by  $\sim 5$  Ma, the first between 83 and 75 Ma, and the second between 70 and 60 Ma. Stratigraphic evidence indicates that the latter episode included at least four separate periods of thrust motion.

The magnitude and decreasing trend of tectonic subsidence in the Axhandle basin agrees well with other tectonic subsidence curves calculated for other localities within central Utah (figure 11; Heller et al. 1986; Cross 1986). These studies attributed rapid tectonic subsidence between 90 and 74 Ma (Heller et al. 1986) or between 97 and 74 Ma (Cross 1986) to emplacement of the Canyon Range, Pavant, and Nebo thrust sheets. These thrust sheets, comprising of Precambrian and Paleozoic cover rocks, are presently exposed  $\sim 30$  km west of the Axhandle basin (figure 1). Field relations, supported by sparse biostratigraphic control, also indicate that emplacement of these thrust sheets ceased by  $\sim 75$  Ma (Lawton 1985; Villien and Kliegfield 1986); thus the emplacement of major cover thrust sheets shortly predated or was coeval with initial motion on the Gunnison thrust system. Tectonic subsidence during subsequent deposition in the Axhandle basin may have been produced by other sources of crustal loading. Elastic-plate theory suggests that the basin margin structures are too narrow ( $\sim 10$  km) to produce significant tectonic subsidence on lithosphere with an effective elastic thickness of  $\sim 20$  km (Reynolds et al. 1991, their figure 11; Jordan 1981). The San Rafael Swell, a basement-involved upwarp with an axis  $\sim 100$  km east of the Axhandle basin, is of sufficient magnitude and width to cause tectonic subsidence within the basin. It is, however, also possible for this structure to have produced a flexural bulge and hence uplift in the area of the basin (calculated following Angevine et al. 1988 p. 32–33). The San Rafael Swell is inferred to have been active be-

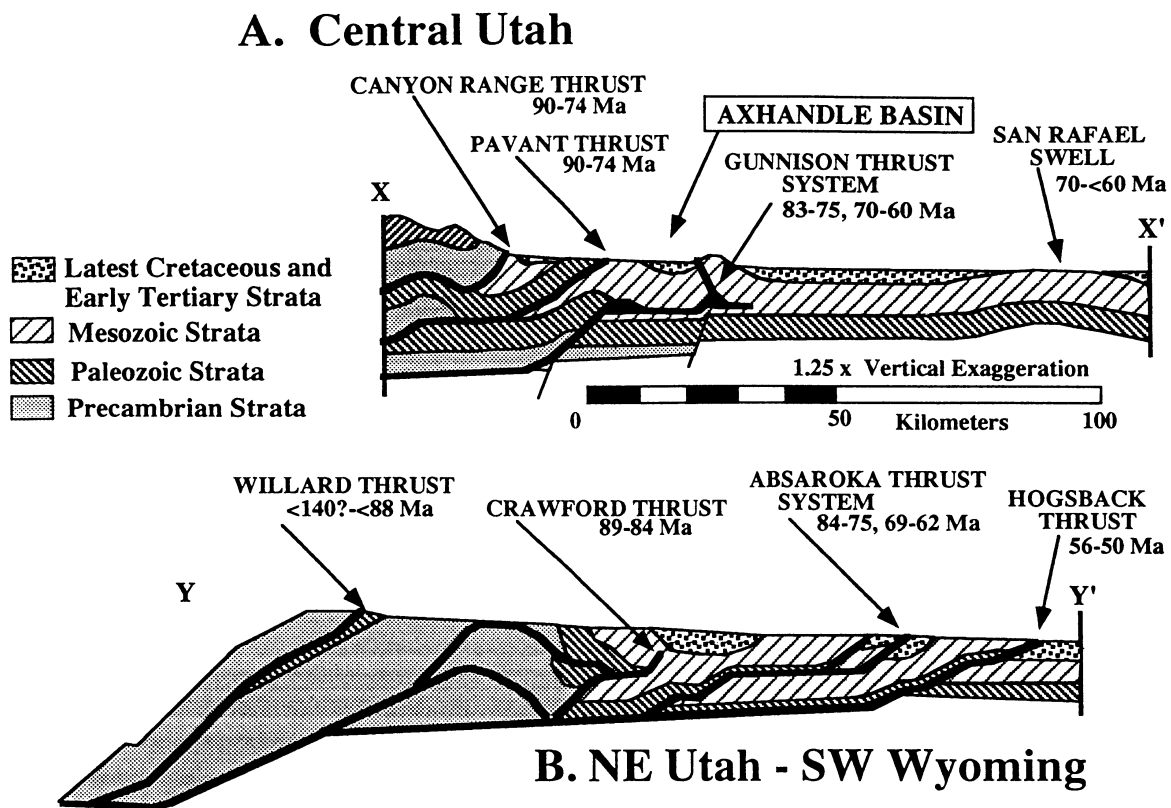


**Figure 12.** Comparison of regional cross sections of different salients of the thrust belt in Central and North Eastern Utah (after Lawton and Trexler 1991 and DeCelles 1994, respectively). The locations of the cross sections are separated by ~300 km (figure 1a). Stratal ages are indicated in the key. Late Cretaceous and Early Tertiary strata in central Utah are represented by the North Horn Formation. The timing of motion on each thrust is indicated. The Gunnison and Absaroka thrust systems occupy similar positions within the overall thrust wedge, and were active during similar periods. Cross section topographies are reconstructed paleotopographies.

tween ~70 and 60 Ma, based on a regionally developed erosional unconformity (Franczyk and Pitman 1991; Franczyk et al. 1991); thus uplift on the structure is, within dating uncertainties, synchronous with the second period of motion on the Gunnison thrust system.

Thus thrusting in central Utah migrated ~140 km in ~40 Ma, an average rate of ~3.5 mm/yr (figure 1). The Gunnison thrust system was episodically re-activated over a 24 m.y. period. As shown by Lawton and Trexler (1991), this period compares to a maximum period of 34 m.y. during which major thrust sheets were emplaced to the west. Age constraints demonstrate that shortening was synchronous on separate contractional structures. In the case of the Gunnison thrust system and San Rafael Swell, these structures had very different structural styles. Periods of regional structural quiescence (e.g., 75–70 Ma) additionally suggest that

the entire thrust wedge was only episodically active.

#### Comparison to the Thrust Belt in NE Utah and Wyoming

The history of thrust wedge evolution in central Utah is remarkably similar to that seen ~250–350 km to the north in NE Utah and Wyoming (P. DeCelles pers. comm. 1993). Individual thrusts are not, however, continuous between these two locations (Allmendinger et al. 1986; Cross 1986), which comprise separate salients of the thrust belt. Estimates of total shortening of between 100 and 120 km (DeCelles 1994; Allmendinger et al. 1986), across the entire thrust belt are comparable at each location, as is the number (four) of major contractional structures. Both the Gunnison and Absaroka thrust systems lie to the east of two thrust sheets

that involve cover rocks and account for the majority of total thrust belt shortening (figure 12). The timing of motion on the Gunnison and Absaroka thrust systems is identical within dating uncertainties. These periods of motion occurred during, or very shortly after, emplacement of the major thrust sheets to the west, but before shortening on structures to the east (figure 12). The potentially earlier age of initial thrusting in NE Utah, and the basement-involved character of the San Rafael structure, are the most significant differences between the two localities. There are also broad similarities in the passive margin stratal wedge that the thrust belt at both localities were developed within.

The synchronicity of deposition and erosion above the Absaroka and Gunnison thrusts between 84 and 60 Ma is surprising, as these localities occur in entirely different salients of the Sevier thrust belt (Allmendinger et al. 1986; Cross 1986). Whether a locality above a thrust is net-erosional or net-depositional is likely to reflect a balance between flexural subsidence and structural uplift. Estimates of total shortening of ~30 km on the Absaroka thrust (DeCelles 1994) are significantly greater than those of ~5 km for the Gunnison thrust system (Lawton 1985). Presumably greater flexural loading adjacent to the Absaroka thrust offset a greater structural uplift, although differ-

ences in the angles of the thrust faults underlying the two basins may also have been a factor.

The broadly uniform evolution of the thrust wedge, comprising of different thrust systems located over 300 km along strike, suggests that the contractional stresses driving the thrust wedge were also uniform over this distance. Evolution of the thrust wedge is demonstrated to consist of episodes of reorganization, by motion on multiple thrust structures, separated by periods of quiescence. These episodes may result from exceeding critical thresholds for wedge development, or from fluctuations in the magnitude of contractional stresses driving the thrust belt. The period of these episodes is typically around 5 m.y.

#### ACKNOWLEDGMENTS

This research was supported by National Science Foundation grants to DWB (EAR-8905053) and to TFL (EAR-8904835), by the Dept. of Geological Sciences at USC, and by the Geological Survey Evolution of Sedimentary Basins Program. Similarities between the evolution of the Sevier thrust belt in Central Utah and NE Utah-Wyoming were pointed out by Peter DeCelles. Reviews by Peter DeCelles and two anonymous reviewers substantially improved the manuscript.

#### REFERENCES CITED

- Allen, P. A., and Allen, J. R., 1990, *Basin Analysis: Principles and Applications*: Oxford, Blackwell Scientific Publications, 451 p.
- Allmendinger, R. W.; Farmer, H.; et al., 1986, Phanerozoic tectonics of the Basin and Range—Colorado Plateau transition from COCORP data and geologic data: a review, *in* Barazangi, M., and Brown, L., eds., *Reflection Seismology: The Continental Crust*: Am. Geophys. Union Geodynam. Ser., No. 14, p. 257–267.
- Angevine, C. L.; Heller, P. L.; and Paola, C., 1988, Quantitative sedimentary basin modeling: Am. Assoc. Petrol. Geol. Short Course Notes, 133 p.
- Cande, S. C., and Kent, D. V., 1992, A new geomagnetic polarity time-scale for the late Cretaceous and Cenozoic: *Jour. Geophys. Res.*, v. 97, p. 13,917–13,953.
- Cross, T. A., 1986, Tectonic controls of foreland basin subsidence and Laramide style deformation, Western U.S., *in* Allen, P. A., and Homewood, P., eds., *Foreland basins*: Int. Assoc. Sed. Spec. Pub. 8, p. 15–39.
- DeCelles, P. G., 1994, Late Cretaceous–Paleocene synorogenic sedimentation and kinematic history of the Sevier thrust belt, northeast Utah and southwest Wyoming: *Geol. Soc. America Bull.*, in press.
- Diehl, J. F.; McClannahan, K. M.; and Bornhorst, T. J., 1988, Paleomagnetic results from the Mogollon volcanic field, southwest New Mexico, and a refined mid-Tertiary reference pole for North America: *Jour. Geophys. Res.*, v. 95, p. 4869–4879.
- Fisher, R., 1953, Dispersion on a sphere: *Proc. Royal Soc. (London) Series A*, v. 217, p. 295–305.
- Fouch, T. D.; Lawton, T. F.; et al., 1982, Chart showing preliminary correlation of major Albian to middle Eocene rock units from the Sanpete Valley in central Utah to the Book cliffs in eastern Utah, *in* Nielson, D. L., ed., *Overthrust Belt of Utah*: Utah Geol. Assoc. Pub. 10, p. 267–272.
- Franczyk, K. J.; Hanley, J. H.; Pitman, J. K.; and Nichols, D. J., 1991, Paleocene depositional systems in the western Roan Cliffs, Utah, *in* Chidsey, T. C., ed., *Geology of east-central Utah*: Utah Geol. Assoc. Pub. 19, p. 111–127.
- , and Pitman, J. K., 1991, Latest Cretaceous non-marine depositional systems in the Wasatch Plateau area: reflections of foreland to intermountain basin transition, *in* Chidsey, T. C., ed., *Geology of east-central Utah*: Utah Geol. Assoc. Pub. 19, p. 77–93.
- Freeze, R. A., and Witherspoon, P. A., 1967, Theoretical analysis of regional groundwater flow. 2 Effect of wa-

- ter table configuration and subsurface permeability variation: *Water Resour. Res.*, v. 3, p. 623–634.
- Gile, L. H.; Peterson, F. F.; and Grossman, R. B., 1966, Morphologic and genetic sequence of carbonate accumulation in desert soil: *Soil Sci.*, v. 101, p. 347–360.
- Greisbach, F. R., and MacAlpine, S. R., 1973, Reconnaissance palynology and micropaleontology of the late Cretaceous–early Tertiary North Horn Formation, Central Utah: *Geol. Soc. America Abs. with Prog.*, v. 5, p. 483.
- Harland, W. B.; Armstrong, R. L.; et al., 1990, *A Geologic Time Scale 1989*: Cambridge, Cambridge University Press, 263 p.
- Heller, P. L.; Bowdler, S. S.; et al., 1986, Time of initial thrusting in the Sevier orogenic belt, Idaho-Wyoming and Utah: *Geology*, v. 14, p. 388–391.
- Hobbs, R. S., 1989, The physical and magnetic polarity stratigraphy of the Upper Cretaceous–Lower Tertiary North Horn and Flagstaff Formations, Gunnison Plateau, central Utah: Unpub. M.S. Thesis, University of Southern California, Los Angeles.
- Jacobson, S. R., and Nichols, D. J., 1982, Palynological dating of syntectonic units in the Utah-Wyoming thrust belt: the Evanston Formation, Echo Canyon conglomerate, and Little Muddy Creek conglomerate, in Powers, R. G., ed., *Geologic Studies of the Cordilleran Thrust Belt*: Denver, Rocky Mtn. Assoc. Geol., p. 735–750.
- Jordan, T. E., 1981, Thrust loads and foreland basin evolution, Cretaceous, western United States: *Am. Assoc. Petrol. Geol. Bull.*, v. 65, p. 2506–2520.
- Johnson, N. M.; Opdyke, N. D.; and Lindsay, E. H., 1975, Magnetic polarity stratigraphy of Pliocene-Pleistocene deposits and vertebrate faunas, San Pedro Valley, Arizona: *Geol. Soc. America Bull.*, v. 86, p. 5–12.
- La Rocque, A., 1960, Molluscan Faunas of the Flagstaff Formation of central Utah: *Geol. Soc. America Mem.* 78, 100 p.
- Lawton, T. F., 1985, Style and timing of frontal structures, thrust belt, central Utah: *Am. Assoc. Petrol. Geol. Bull.*, v. 69, p. 1145–1159.
- , Talling, P. J.; et al., 1994, Structure and stratigraphy of Upper Cretaceous and Paleogene strata, eastern San Pitch Mountains, Utah: sedimentation at the front of the Sevier orogenic belt: U.S. Geol. Survey Prof. Paper, in press.
- , and Trexler, J. H., 1991, Piggyback basin in the Sevier orogenic belt, Utah: implications for development of the thrust wedge: *Geology*, v. 19, p. 827–830.
- Meghraoui, M.; Jaegy, R.; Lammali, K.; and Albaredé, F., 1988, Late Holocene earthquake sequences on the El Asnam (Algeria) thrust fault: *Earth Planet. Sci. Lett.*, v. 90, p. 187–203.
- Peck, R. E., and Reker, C. C., 1948, Eocene charophyta from North America: *Jour. Paleont.*, v. 22, p. 85–90.
- Reynolds, D. J.; Steckler, M. S.; and Coakley, B. J., 1991, The role of sediment load in sequence stratigraphy: the influence of flexural isostasy and compaction: *Jour. Geophys. Res.*, v. 96, p. 6931–6949.
- Rich, T. H. V., and Collinson, J. W., 1973, First mammalian fossils from the Flagstaff Limestone, central Utah: *Vulpavis australis* (Carnivora Miacidae): *Jour. Paleont.*, v. 47, p. 854–860.
- Schwanns, P., 1988, Stratal packages at the subsiding margin of the Cretaceous foreland basin: Unpub. Ph.D. dissertation, Ohio State University, Columbus (2 volumes), 447 p.
- Sclater, J. G., and Christie, P. A. F., 1980, Continental stretching: an explanation of the post mid-Cretaceous subsidence of the central North Sea basin: *Jour. Geophys. Res.*, v. 85, p. 3711–3739.
- Spieker, E. M., 1949, Sedimentary facies and associated diastrophism in the upper Cretaceous of central and eastern Utah: *Geol. Soc. America Mem.* 39, p. 55–81.
- Standlee, L. A., 1982, Structure and stratigraphy of Jurassic rocks in central Utah: their influence on tectonic development of the Cordilleran foreland thrust belt, in Powers, R. B., ed., *Geologic Studies of the Cordilleran Thrust Belt V. 1*: Denver, Rocky Mtn. Assoc. Geol., p. 357–382.
- Stanley, K. O., and Collinson, J. W., 1979, Depositional history of Paleocene–lower Eocene Flagstaff Limestone and coeval rocks, central Utah: *Am. Assoc. Petrol. Geol. Bull.*, v. 63, p. 311–323.
- Talling, P. J., 1992, Magnetostratigraphically constrained evolution of the 75 to 51 Ma Axhandle thrust-top basin, central Utah: Unpub. M.S. thesis, University of Southern California, Los Angeles, 217 p.
- , and Burbank, D. W., 1994, Assessment of uncertainties in magnetostratigraphic dating of sedimentary strata, in Aissaoui, D. M.; McNeill, D. F.; and Hurley, N. F., eds., *Applications of paleomagnetism to sedimentary geology*: SEPM Spec. Pub. 50, in press.
- Tomida, Y., and Butler, R. F., 1980, Dragonian mammals and Paleocene magnetic polarity stratigraphy, North Horn Formation, central Utah: *Am. Jour. Sci.*, v. 280, p. 787–811.
- Villien, A., and Kliegfeld, R. M., 1986, Thrusting and synorogenic sedimentation in central Utah, in Peterson, J. A., ed., *Paleotectonics and sedimentation in the Rocky Mountain Region, United States*: *Am. Assoc. Petrol. Geol. Mem.* 41, p. 281–308.
- Zijderveld, J. D. A., 1967, A.C. demagnetization of rocks: analysis of results, in Collinson, D. W.; Creer, M. A.; and Runcorn, S. K., eds., *Methods in Paleomagnetism*: New York, Elsevier, p. 254–286.